Chapter-1

1.1 Raman Spectroscopy

Electromagnetic radiation-matter interaction involves numerous phenomena. Examples of light absorption and subsequent emission by materials include fluorescence and phosphorescence. Predominantly, elastic scattering of light where the frequency of light does not change involves Rayleigh scattering by atoms, molecules, or phonons as well as Mie scattering by dust particles. Inelastic scattering, where the frequency of the light changes often referred to as Brillouin scattering by acoustic waves in crystals, Compton scattering by charged particles, and Raman scattering by molecules or phonons. Raman scattering process involves a resonance with a vibrational state, where a molecule must undergo a change in its polarizability during vibration [1]. Using quantum theory, Smekal provided the theoretical prediction of Raman scattering of light by molecules for the first time in 1923 [2] and experimentally observed in liquid by C.V. Raman and Krishnan in 1928 [3]. At the same time, Landsberg and Mandelstam observed the same finding in quartz crystal [4]. Raman's pioneering discovery in light scattering was carried out using sunlight as an excitation source, telescope objective, filters, and first visual observation of color changes in the scattered light was discovered as a 'new type of secondary radiation' [3]. Afterwards, C.V. Raman and Krishnan recorded the spectrum of some 60 liquid samples using a mercury lamp and quartz spectrograph. In 1930, Raman received the physics Nobel Prize for his discovery, and the phenomenon got named as the 'Raman effect' in honor of Sir C.V. Raman. Following the publication of Raman's note in the Nature, over 60 studies discussing

the Raman effect were published, and worldwide, more than 1700 papers on Raman spectroscopy were published in 1939 [5]. Based on data from 1982 to 2005, there were over 4200 published papers overall, with an average of 1800 published papers annually in this field [6].

'Raman effect' was described when incident photons interact with the molecules of material scattered elastically or inelastically. Most of the photons are scattered elastically, which have the same wavelength as the incident photon, i.e., Rayleigh scattering while a small fraction of inelastically scattered photons have shift in wavelength than incident radiation [1]. When the scattered photons are lower in energy than the incident photon, the shift in energy is described as Stokes Raman scattering. Conversely, when the scattered photons are higher in energy compared to the incident photon, the energy shift is described as anti-Stokes Raman scattering [5, 7–9] as shown in **Figure 1.1**. This energy shift depends upon the chemical structure of the molecules, resulting in Raman scattering that provides the information about the molecules. The shift in angular frequency after scattering can be defined as $\omega_s = \omega_p \pm \omega_o$ ($\omega = 2\pi\nu$). Where, ω_p and ω_o denotes the angular frequency of molecular vibration and incident photons. Interaction of incident photons with the vibrational or rotational energy levels of the molecules, referred to the vibrational or rotational Raman spectroscopy [1].

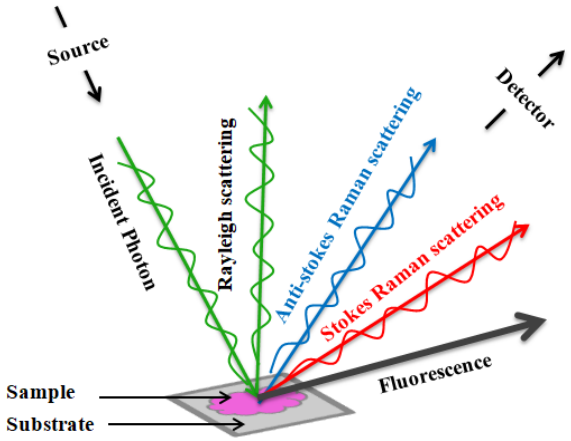

Figure 1.1 *Schematic showing scattering of light on the surface of sample after laser irradiation [9]*

1.2 Theory of Raman spectroscopy

A succinct explanation of the theory of Raman scattering is given in the following subsections. The finding could be interpreted using either the classical wave approach or the following quantum mechanical feature, as given below.

1.2.1 Classical theory of Raman scattering

According to classical theory, Raman scattering is based upon the change in the polarizability of a molecule [10–11]. When any sample is irradiated by light, the polarizability $\vec{\alpha}$ gets induced in the molecular via interaction of the oscillating electric field of incident electromagnetic radiation $\vec{E}$. The strength of the induced bulk polarization $\vec{P}$ is the product of $\vec{\alpha}$ and the incident radiation $\vec{E}$ denoted by mathematical expressions,

$$\vec{P} = \vec{\alpha}\vec{E} \quad (1)$$

Incident electric field can be expressed as [11],

$$\vec{E} = \vec{E}_0 \mathrm{Cos} 2\pi\nu_0 t \quad (1.2)$$

Where, ν_0 is the frequency of the incident radiation, time t and maximum field strength $\vec{E}_0$. Generally, the molecular vibrations are consist of normal coordinate modes q which varies periodically with the vibrational frequency ν_m is represented by [10-11],

$$q = q_0 \mathrm{Cos}\, 2\pi\nu_m t \quad (1.3)$$

Where, q_0 is the magnitude of normal mode. The polarizability of electrons in molecules can be modulated by molecular vibration according to [10–11],

$$\vec{\alpha} = \overrightarrow{\alpha_0} + \left(\frac{\delta\vec{\alpha}}{\delta q}\right)_0 q + \ldots\ldots\ldots\ldots \quad (1.4)$$

Where $\overrightarrow{\alpha_0}$ is the polarizability of the molecule in its equilibrium position, $(\delta\vec{\alpha}/\delta q)_0$ is the derivative of the polarizability with respect to the normal vibration mode at the equilibrium position [11-12]. From equation (1), (1.2), (1.3) and (1.4)

$$\vec{P} = \vec{E}_0 \mathrm{Cos} 2\pi\nu_0 t + \frac{1}{2}\left[\left(\frac{\delta\vec{\alpha}}{\delta q}\right)_0 q_0 \mathrm{Cos}\{2\pi(\nu_0 - \nu_m)t\} + \left(\frac{\delta\vec{\alpha}}{\delta q}\right)_0 q_0 \mathrm{Cos}\{2\pi(\nu_0 + \nu_m)t\}\right] \quad (1.5)$$

Equation (1.5) reveals three different scattered frequencies. ν_0 represents the unchanged frequency of incident photon after interacting with the molecule i.e. the first term corresponds to Rayleigh scattering. The second term in the above equation, i.e., Raman scattering with the decrease in frequency ($\nu_0 - \nu_m$) is known as the Stokes shift, while the term with the increased frequency ($\nu_0 + \nu_m$) represent anti-Stokes shift frequencies. Thus, the change in incident radiation in terms of Stokes and anti-Stokes shift can be used to measure the vibrational frequencies of a chemical bond [10–13].

1.2.2 Quantum theory of Raman scattering

Raman scattering can be interpreted more comprehensively by applying quantum theory. According to quantum theory, Raman scattering arises due to the collision between incident photon and molecules of the sample. The quantum theory states inelastic collision occurs when a photon with radiation of frequency v and energy hv, collides with a molecule, and the excitation places the molecule into the virtual state for a short time before the photon is emitted [10, 14]. The photon is scattered with energy h ($v_0 \pm v_m$), and the scattered frequency will be ($v_0 \pm v_m$) accordingly if the molecules acquire and vanish energy during an inelastic collision. Here, ΔE stands for the energy difference between two permitted states [10, 14]. Rayleigh scattering occurs when incident and scattered photon have the same energy, as discussed in the above section classically [10, 14]. If the scattered photon exhibits the shift in energy with the value $\Delta E = hv_m$, which is referred to as Stokes shift or anti-Stokes shift of Raman scattering [10, 14, 15]. Types of scattering are represented in **Figure 1.2**. Since the majority of molecules are in the ground state at room temperature according to Boltzmann distribution law, so there is a higher probability of Stokes scattering than that of anti-Stokes scattering of photons during Raman measurements [11]. In Raman scattering, intensity is directly proportional to the change in the polarizability of molecules.

The Raman process is often carried out using optical fields that resonate with electronic transitions, and the low-frequency Raman resonances represent vibrational motions and low-lying electronic excitations [16]. Spontaneous Raman

Scattering (SRS) or coherent Raman Scattering (CRS) are the methods for observing Raman resonances. Light-matter interaction also involve a third order four wave mixing (4WM) process, in which three incoming laser fields with wave vectors k_1, k_2 and k_3 and three frequencies $\omega_1, \omega_2,$ and ω_3 respectively, interact with the non-linear third order susceptibility $\chi^{(3)}$ of material to coherently generate single field at frequency ω_s. The wavelength of light can be selected so that the emitted light is spectrally distinct from the incident radiation, which makes it easier to identify the signal with wave vector k_s [16]. Where,

$$k_s = \pm k_1 \pm k_2 \pm k_3 \tag{1.6}$$

and

$$\omega_s = \pm \omega_1 \pm \omega_2 \pm \omega_3 \tag{1.7}$$

Equation 1.6 indicates the linear combination of wave vector k_s and frequencies ω_s and different choice of these terms (positive or negative) posses different types of 4WM process. 4WM signal is sensitive for both electronic as well as vibrational properties of the materials. This specific selection of frequencies is featured as spatial type of 4WM i.e. CARS (coherent anti-Stokes Raman scattering) kind of interaction, which was reported by Maker and Terhune in 1965 for the first time. CARS, is the coherent analogue of spontaneous Raman spectra and it has significance role in the field of biological imaging, nanomaterial or nanostructures [16].

Vibrational Raman spectra

Vibrational Raman spectra obtained due to the collision between the

incident photons and the molecules of the material. After the collision, molecule will undergo a change in energy and according to law of conservation the new energy state in a molecule can be described [17] by the equation as given below,

For, v = velocity of molecule

m = Mass of the molecule before collision with photon

E_β = Energy of the molecule before collision

hν = Energy of the incident photon

$$E_\beta + \tfrac{1}{2} mv^2 + h\nu = Eq + \tfrac{1}{2} mv'^2 + h\nu' \quad (1.8)$$

Where, v' = Velocity of the molecule after the collision

Eq = Energy after the collision

ν'= Frequency of the photon after the collision

Since the change in velocity is practically negligible, thus the above equation can be written as

$$E_\beta + h\nu = Eq + h\nu' \quad (1.9)$$

$$\nu' = \frac{\nu + E_\beta + E_q}{h} \quad (1.10)$$

$$\nu' = \nu + \Delta\nu \quad (1.11)$$

Equation (1. 10) resulted in three cases,

(a) If E_β = Eq (Rayleigh scattering) the frequency difference (Raman shift), Δν [i.e. $(E_\beta - Eq) / h] = 0$. It shows ν' = ν and referred to as a photon-deflecting molecule that does not take the photon's energy. Rayleigh scattering is comparable to this elastic collision [17].

(b) If $E_\beta >$ Eq (anti-Stokes shift) then $\nu' > \nu$ which corresponds to the anti-Stokes shift. It follows that when the molecule was previously energized, some of its internal energy was transferred to the incident photon. Thus, the photons that are scattered therefore have more energy [17].

(c) If $E_\beta <$ Eq (Stokes shift) and $\nu' < \nu$. This corresponds to Stokes shift. The scattered photon will have the lowest energy since the molecule has absorbed some of the energy from the photon. According to equation (1.9), the Raman effect's difference in frequency ($\nu - \nu'$) between incident and scattered photons corresponds to the molecule's characteristic frequency 'ν_c'. Thus, the equation can be used to determine the characteristic frequency

$$\nu' - \nu = \pm \nu_c \approx (\Delta\nu) \qquad (1.12)$$

Equation (1. 12) demonstrate that the difference in frequency ($\nu'-\nu$) between the incident and scattered photon in the Raman effect depicts the characteristic frequency ν_c of the molecule [17].

In other words, the frequency of the scattered radiation only depends on the difference between the initial and final states of the quantum, and the initial and final states of the molecule must differ for there to be an energy transfer between them. Thus, this difference is independent to the laser wavelength and is only related to the energy characteristics of the measured molecular vibrations.

Invention and the abundance of laser as an excitation source of Raman spectrometer has resulted in various avatars of Raman spectroscopy [5]. Ninty five

years later, due to a unique set of energy levels for Raman scattering of molecules, it has become foremost technique among the other analytical techniques with the advent laser, filters, computer etc. Now, over twenty-five different types of Raman spectroscopy tools are recognized [1, 18].

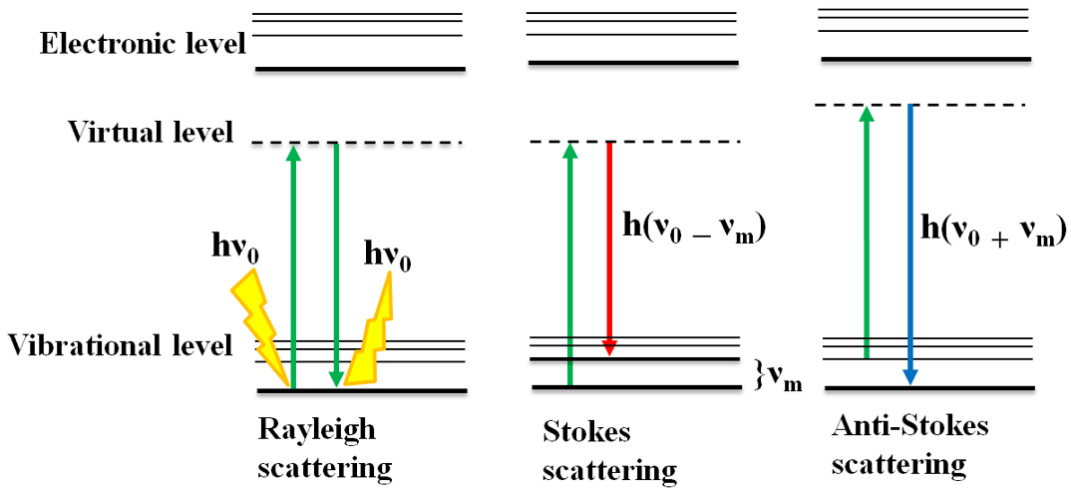

Figure 1.2 *Energy levels diagram of Rayleigh and Raman scattering (Stokes and anti-Stokes scattering)*

Raman technique also possesses other intrinsic advantages such as (a) non-invasive and lable-free tool, (b) Analysis of organic, inorganic materials, and biological samples, since water has relatively weak Raman scattering, (c) No sample preparation and (d) Potential of multi-molecule detection i.e. detection of different analytes simultaneously [10, 14, 18–19]. Limitations of Raman scattering are that it is a very weak phenomena only one in a million photons is Raman scattered as compared to Rayleigh scattering (~1 in 10^4 photons), and the interference from fluorescence [10, 14, 18–19]. Since the sensitivity of the 'Raman effect' is so low, which make it challenging to measure low concentrations of a sample for

quantitative analysis, typically analytical concentrations higher than 0.01 M are required to record conventional Raman spectra [20]. Thus, Raman spectroscopy didn't gain prominence as an analytical technique until certain discovery was made to enhance the signals.

1.3 Surface enhanced Raman Spectroscopy (SERS)

Fleishman and co-workers observed the significant amplification in Raman signal of pyridine adsorbed onto the roughened silver surface in 1974 for the first time [21], and this finding has drawn substantial following as many analytes on the rough surface due to larger surface area with the number of citation over 6000 times for initial publication. The enhancement in Raman signal due to the rough metal surface is named surface enhanced Raman spectroscopy (SERS) [22]. The reason behind the enhancement in Raman signal because of an increase in the number of adsorbates was not enough to explain. In 1977 one group, Jeanmaire and Van Duyne, suggested an electric field effect [23], while another group, Albrecht and Creighton, independently proposed the chemical effect for the observed Raman enhancement [24]. Surface-enhanced Raman scattering (SERS) was at it's infancy with this prediction. In 1997, SERS received much attention, with the report by Kneipp et al. [25], and Nie and Emory [26] who independently observed SERS of single molecule on nanomaterials with huge enhancement in Raman signal, and this trend got popular with the increased number of citations over the years. SERS is a prominent spectroscopic tool in which Raman signals are largely enhanced, and the observed enhancement factor is more than 10^6, when analyte molecules are in close vicinity

of the metal surfaces. SERS is a highly active research area and has attracted much attention in multidisciplinary fields like photonics, analytical, explosive or chemical weapons, biology or biomedical, and pollutants applications, etc. [27–32]. The development and availability of nanoscience facilitated the fast growth of SERS because they can serve as an effective substrate to enhance the Raman signals [27–32]. Moreover, the significant contribution of Raman intensity enhancement is arguably explained via two mechanisms such as electromagnetic enhancement (EM) and charge transfer mechanism (CM). Since polarizability (α) and the strength of the incident electromagnetic field (E) are combined to form the induced dipole moment, which is precisely proportional to both of these factors, it is caused by the enhancement in both of these mechanisms [32–35].

Schatz groups have provided the results of several further trials that immediately followed to discover experimental conditions that affect improvement [36–37]. The molecular identity was found to have a less significant impact on enhancement than surface modification (i.e., roughness) and substrate dielectric properties. These experimental results sparked many inquiries into the underlying theories of the surface-enhancement mechanism. Optimization of enhancement is necessary for SERS to be properly utilized in analytical chemistry, and this can only be accomplished by understanding the enhancing mechanism. Although there are still many gaps and competing models, theoretical progress in the mechanical foundations of SERS is continually being made [36–37]. On the other hand, the electromagnetic mechanism attempts to elaborate amplification by changes in the localized field that the adsorbate at the enhancing substrate surface experiences.

Although the explanation of the chemical mechanism is more controversial because it is thought to be result from a resonance charge-transfer state between the molecule adsorbed and substrate. It is consistent with the fact that SERS depends on the dielectric characteristics and substrate's roughness, where CM also has a significant role in the enhancement even though EM contributes to the dominant surface enhancement more than CM [32, 38–40].

(a) Electromagnetic effect

Gersten and Nitzan were the first who study the SPR contributions in SERS using a model as metal ellipsoid or semi-ellipsoid [39]. In SERS, enhancement of the local electric field at adsorbed molecule arises due to the plasmonic excitation on the surface of the substrate. The collective oscillations of electrons known as surface plasmons are caused by the incident photon's time-varying electric field, and the quasi-particles of these excitation known as localized surface plasmon, was first observed by Moskovits [41]. Surface plasmons are localized on roughened nano-sized structures or curved structures where the excitation of surface plasmons amplifies the local electromagnetic field of light, leading to the enormous enhancement of Raman signals, as depicted in **Figure 1.3**. Surface plasmon, or localized surface plasmon resonance (LSPR), which is carried through free electrons, provides localized optical fields [41–42]. The magnitude of the local electric field in SERS of the adsorbed molecule on the metallic surface depends upon several parameters: Particle dimension, dielectric property, consequences of dipolar re-radiation, adsorption molecule geometries, polarization, and wavelength of incident

radiation [33, 43]. The enormous surface-enhanced Raman effect, also called "plasma resonance-enhanced Raman," is produced by the surface plasmon resonance of a metallic substrate or by Mie scattering. Creighton and coworkers concluded that whatever materials worked best depended on the dielectric nature of the metal substrate (such as Ag, Au, or Cu) [42]. Since the local field enhancement arising from the excitation of plasmon can generate a strong field, it is believed that the electromagnetic enhancement mechanism has a dominant contribution to the SERS signal [33]. In this approach, it is typically assumed that the SERS signal is strengthened by a factor proportional to the fourth-power of the electric field enhancement, (E^4) [39].

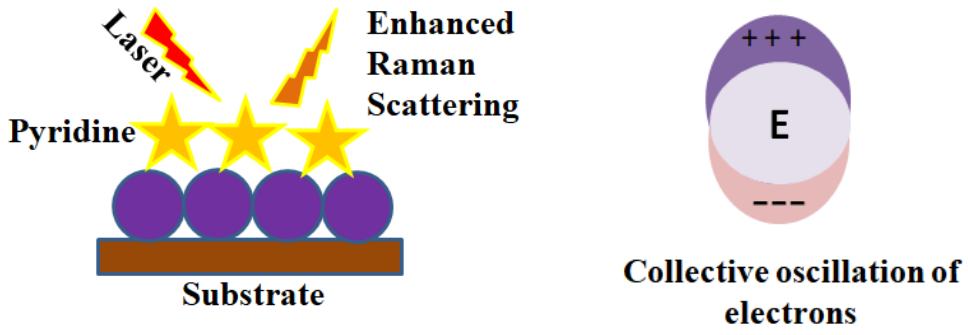

Figure 1.3 *schamatic identifying of localized surface plasmon*

The interaction of light with a spherical particle whose dimension is substantially smaller than the wavelength of light is considered to relate the LSPR frequency of a metal nanoparticle (NP) to the dielectric constant. In this case, considering that the electric field of light is constant, electrostatics governs the interaction rather than electrodynamics [44]. This is frequently referred to as the quasistatic approximation,

or dipole approximation. Consider a quasistatic method using a spherical nanoparticle with radius 'a' that is subjected to z-polarized light with a wavelength in the long wavelength limit and the dielectric constant of metal is $\varepsilon_i$and for medium surrounding the sphere is ε_o. The electric field (E) around the particle can be determined by calculating the electrostatic Laplace's equation. When an electromagnetic field is present outside of the particle, the resulting solution, E_{out} [45], is given as,

$$E_{out}(x,y,z) = E_0\hat{z} - \alpha E_0\left[\frac{\hat{Z}}{r^3} - \frac{3Z}{r^5}(x\hat{x} + y\hat{y} + z\hat{z})\right] \quad (1.13)$$

Where r is the radial distance, $x, y, z$and $\hat{x}, \hat{y}, \hat{z}$ are cartesian coordinates and unit vectors respectively, and α denotes the polarizability metal sphere given as $\alpha = ga^3$. The value g can be defined as, $g = \frac{\varepsilon_i - \varepsilon_o}{\varepsilon_i + 2\varepsilon_o}$. From equation (1.13), the maximum enhancement will obtained when the denominator of g tend to zero (i.e.$\varepsilon_i \approx -2\varepsilon_o$). In Raman scattering, there is a linear relation between scattered intensity and intensity of incident field E_0^2. Since this field intensity is amplified at the nanoparticle surface, the Raman intensity is consequently correlated with the square of E_{out} calculated at the metal surface (r = a). For a small metal from equation (1.13) and value of g,

$$|E_{out}|^2 = E_0^2[|1-g|^2 + 3Cos^2\theta(2Re(g) + |g|^2)] \quad (1.14)$$

Where, θ is the angle between incident field vector and position vector of molecule on surface. When g value is high, the averaged radial intensity is $|E_{out}|^2 = 2E_0^2|g|^2$. The overall term for amplification of the incident field is provided by equation (1.14), which also suggests that the emission of light from the dipole in Raman

scattering can be amplified. So the approximate electromagnetic enhancement [45] can be expressed as

$$EM_{EF} = \frac{|E_{out}|^2 |E'_{out}|^2}{|E_0|^4} \quad (1.15)$$

Moreover, nuemerical calculation for enhancement factor is based upon analytical theory i.e. Mie theory or quasistatic approximation. Genarally, classical theoretical electrodyanamic method for SERS enhancement factor of resonant molecule on nanostructure surface is goverened by discrete dipole approximation (DDA), and finite difference time-domain FDTD calculation. Among them FDTD calculation is widely used in SERS to determine local electric field by Maxwell's equations [36, 46].

Where, $|E'_{out}|$ or $|E'_{loc}|$ is the local electric field of Raman enhancement.The enhancement factor for a plane wave interacting with the particle replaces the emitted photon enhancement factor, related to the induced dipole's Stokes frequency emission from the adsorbed molecule, to approximate the effects of dipole re-radiation. $|E_{out}| = |E'_{out}|$, i.e., it is highly typical to neglect the distinction between incident (ω_o) and stoke shifted frequency (ω_s) or to assess the improvement in the limit of zero Stokes shift [42, 47]. The expression (1.15) can be written as for maximum enhancement,

$$EM_{EF} = |E_{out}|^4 \quad (1.16)$$

To better understand the electromagnetic enhancement hypothesis, consider a semiconductor material whose surface plasmon resonance increases proportionally to the electron density. In the near-field of microstructure or nanostructure, the

incident plane wave is considerably distorted to fulfill the surface boundary condition [46]. Since the plasmon of semiconducting materials is anticipated to be far from the value for SERS measurement in the visible range, however, the plasmon resonance of semiconductors was found to be capable of showing a strong near-infrared optical absorption for various geometries or nanocrystals with tuned shapes. It could be utilized as a plasmonic sensor for detecting different molecules by SERS. This means their contribution to SERS enhancement was not insignificant [46, 48].

On the other hand, for large dimensions, Mie resonance also has the potential to increase the electric field in semiconductors of nano or microstructures in which metallic plasmon resonance associated with the geometric configurations has significant radial dependency [43]. Additionally, according to the Mie scattering theory, the size or wavelength-dependent spectra of plasmons in semiconductor materials can be evaluated using the complex refractive index. Hayashi et al. were the ones who first applied the Mie scattering theory to semiconducting nanomaterials and noticed the importance of the EM process even for dielectric particles [47, 49].

(b) Chemical effect

The Chemical effect plays a vital role in SERS enhancement because various SERS spectral features can't be explained on the basis of electromagnetic theory [33–35].

Chemical enhancement mechanism (CM) associated with the chemisorption interaction between the molecule adsorbed and the surface of the nano-metal substrate due to the electron transfer that causes a change in polarizability resulting

in amplification of Raman signal of adsorbate or involves a new electronic transition in metal-molecule charge transfer arises in resonance Raman effect [40]. This process includes (a) transfer of electron in the metal-molecule system occurs between the ground state and excited state, (b) Photo-driven charge transfer process contribute in the amplification of Resonance-like Raman scattering when the excitation energy of the incident light is in resonance with the electron transfer energy that can improve the polarizability of the surface complex, (c) the charge transfer phenomenon resulting chemical bond formation occurs between the highest occupied molecular orbital (HOMO) to the lowest unoccupied molecular orbital (LUMO) of the adsorbed molecule, and when the energy level of the adsorbate fall with the proximity to the Fermi level of a metal substrate facilitates the electronic transition [39–46] as shown in **Figure 1.4**.

Formation of the chemical bond, resonance, and photo-induced charge transfer between adsorbate and substrate contributed to CM, and these can affect the orientation or electronic structure of the molecule, causing spectral shifts and change in intensity for different modes of molecules. The magnitude of charge transfer enhancement depends upon the adsorbed molecule or the nature of the molecular states, so the probe molecules must be directly interacted with the metal surface [35–46]. However, the chemical mechanism (CM) contributed to SERS enhancement, but CM is not well defined yet because of its entanglement with electromagnetic enhancement. CM's enhancement of the Raman signal generally contributed about 2 to 4 orders of magnitude [35, 39].

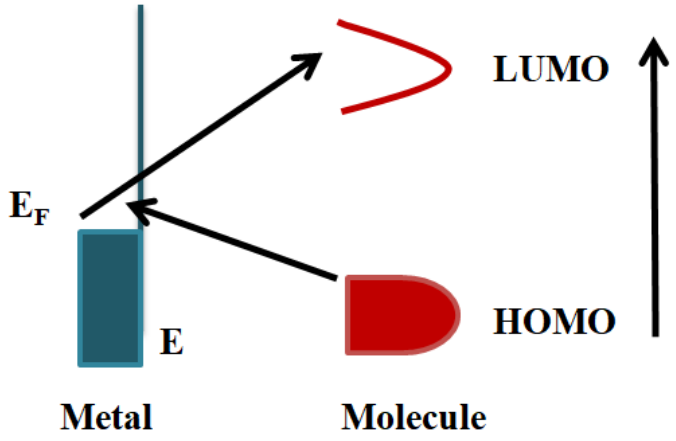

Figure 1.4 *Illustration of typical energy level diagram of adsorbed molecule on SERS substrate*

1.3.1 Plasmon-induced CM

The charge transfer process between plasmon nanomaterial and interacting probe (directly or indirectly) plays a crucial role in both plasmon-induced chemical reaction and CM. Apart from that, surface plasmon resonance may also induce various chemical reactions in the molecule that is adsorbed to the surface of metal nanostructures, causing the formation of new molecules. Based on the mechanism, the primary distinction between them is where the excited carriers go in the final stage. The transferred excited carriers in SERS rapidly decay to the metal or surface complex, intensifying the Raman signal in a resonance-like approach. While in the plasmon-induced chemical reaction, excited carriers that have been transported from the surface plasmon substrate to the analyte take part in the chemical reaction. By prolonging the time duration that excited carriers occupy in the orbital of reactants, it is possible to raise the likelihood of excited carriers in chemical processes. The

plasmon-mediated chemical processes on metal substrate surfaces may open new possibilities for visible-light-driven photocatalytic reactions [50, 51].

p-aminothiophenol (PATP) or p-nitrothiophenol (PNTP) molecules are usually chosen as ideal probe molecules in SERS because it has a high affinity for SERS substrate and these are sensitive to the electronic property of the most metal substrate. It demonstrates the abnormal amplification peaks in SERS observed from ag modes of 4, 4′-dimercaptoazobenzne (DMAB), an oxidative coupling product due to the chemical transformation of PATP or PNTP that may be observed during the SERS measurement. Latter several reports focused on the transfer of probe molecule into a new species on a metal surface [50–53]. Contrary to recent reports, some studies show that PATP has intense SERS peaks without transformation into DMAB, i.e., PATP exhibits genuine SERS spectra on some metal substrates [54–55].

The application of genuine SERS spectra of PATP instead of plasmon-induced chemical reactions is described in chapter 2.

1.3.2 Enhancement factor calculation

Enhancing factor (EF) is a vital parameter to elucidate the experimental measurement of SERS performance. There are several possibilities to define SERS enhancement factors because of diverse conditions observed in SERS, such as a single molecule, multi-molecule, instrument limitation, analyte orientation on the surface, etc. Defining EF with a single definition is impossible. So there is different possibilities in the evaluation of EF, including the enhancement factor for a single molecule, and the most widely used methods as SERS-active substrate enhancement

factor or the analytical enhancement factor to calculate the SERS performance [56] and is defined below.

(a) Based on analytical chemistry

Consider a probe solution of concentration C_{Raman} that produce a Raman signal I_{Raman} under normal condition. For the same probe molecule of concentration C_{SERS}, at identical experimental condition (laser power, laser wavelength, objective lenses, etc.) results in the SERS signal I_{SERS}. The enhancement factor can be expressed as:

$$\mathrm{EF} = \frac{I_{SERS}/C_{SERS}}{I_{Raman}/C_{Raman}} = \frac{I_{SERS}}{I_{Raman}}\frac{C_{Raman}}{C_{SERS}} \tag{1.17}$$

This definition depends upon adsorption of molecule but the quantity of molecules adsorbed is not precisely defined by C_{SERS}. Additionally, the process used to prepare the samples has a significant impact in EF (dipping or drying) [56].

(b) Based on SERS substrate

The most often used formula for SERS enhancement factor is:

$$\mathrm{EF} = \frac{I_{SERS}/N_{SERS}}{I_{Raman}/N_{Raman}} = \frac{I_{SERS}}{I_{Raman}}\frac{N_{Raman}}{N_{SERS}} \tag{1.18}$$

As surface area and excitation intensity are often not uniform across the scattering volume despite ideal conditions, the EF in this case will depend on how these parameters are approximated, where, I_{SERS} is the SERS intensity, I_{Raman} is the Raman

intensity in normal Raman spectrum and N_{SERS} and N_{Raman} are the number of molecules on the SERS substrate and without substrate under laser irradiation, respectively [56].

Therefore, accurate evaluation of EF requires precise measurement of each parameter (I_{Raman}, N_{Raman}, I_{SERS}, and N_{SERS}). Quantifying SERS studies is difficult since exact values are difficult to find, and suitable assumptions must be made. The EF obtained by various research teams may differ remarkably. Additionally, it makes sense to investigate more reliable approaches to calculating SERS performance [56].

1.4 Material selection for SERS substrates

Any material that exhibits plasmonic behavior at the excitation source may act as a SERS substrate, and it has high chemical stability. For example, surface oxidation has the potential to drastically alter the SERS substrate's LSPR characteristics and its interaction with the analyte, which will have a considerable impact on the repeatability of SERS substrates. Coinage metals like silver, gold, and copper are the most often utilized as SERS substrates with outstanding SERS performance. Silver is employed for irradiation from visible to near-infrared regions, while Au and Cu are typically used for red and near-infrared regions. Au and Cu are employed for the red and near-infrared regions. At the same time, silver can be utilized for excitation from the visible to near-infrared regions and displays high plasmonic properties but less chemical stability than Au and Cu [48, 50–52, 54-55]. Transition metals with their alloys have been used as SERS substrates; iron and nickel are prone to corrosion, while platinum and palladium are chemically stable

[57]. Moreover, alkali metals are also applied as SERS but have some limitations because they readily react with air and aqueous medium [58]. Now a day, semiconducting and dielectric materials are widely used as SERS substrates due to their high stability. Semiconducting materials also display plasmonic properties like noble metals and exhibit dimension-dependent LSPR and SERS performance. The changes arise because of the LSPR of the semiconductor's dependence on the free carriers. However, the core characteristics of electronic nature consist of distribution and carrier density, and the activity of plasmonic SERS semiconductors is not well defined yet [37, 46].

SERS active substrate

(a) Coinage metals

Ag, Au, and Cu coinage metals were first observed as substantial SERS active substrates and are now extensively applied in various fields. Gold and silver nanoparticles are the most prominently used SERS active substrate [50–55]. However, there is a possibility of widespread use of Au but its high cost limited their application to some extent. Noble metal silver is also widely used as a SERS substrate due to very high Raman enhancement signal. Although silver cost is only about one percent of the price of gold, the main drawback of silver is that metal has weaker stability, and is easily oxidized in air [50–55]. On the other hand, it was later shown that transition metals and semiconducting materials have the highest amplification ability when applied to Ag nanoparticles, allowing for the practical use of ultrasensitive sensors. Studies have recently concentrated on creating novel

SERS-active substrates, such as porous silicon covered with gold nanostructure and hexagonal patterns on SiO2. These substrates can produce chemical enhancement driven through charge transfer processes or electromagnetic enhancement related to surface plasmon resonances [58].

(b) Transition metals

Tian and the co-authors observed the SERS performance of transition metals (Pt, Ru, Rh, Pd, Fe, Co, and Ni) in 1996 [57]. Their group developed several roughening methods and improved the performance of the Raman microscope, and the observed enhancement factor was $10–10^4$. The theories accounting for the electromagnetic and chemical components described the SERS characteristics of transition metal nano-rod and electrodes. For adsorption of the molecule on the surface, corrosion, and electro-catalysis of transition metals substrate, the SERS on the transition metals were beneficial [58].

(c) Post-transition metals

The sp valence electrons present in the outermost electron shell define post transition metals, which are softer, have higher electronegativity, lower melting and boiling points in comparison to transition metals with gold or silver [59–60]. Semimetals such as Al, Ga, In, Sn, Tl, Pb, and Bi to nanoparticales exhibit plasmonic resonance in the near to far UV range like noble metals (Ag or Au) in the visible region, and have substantial electric field enhancements in the UV region compared to those of gold in the visible range. In the UV region, noble metals don’t exhibit

very good surface plasmons, the opposite trend of semimetals from Au or Ag makes them especially fascinating for sensing applications in SERS field [59–60]. Experimentally adenine, a nucleobase was used as a proof of deep-UV around~250 nm SERS on arrays of aluminum nanoparticles. SERS properties of Ga, In, Sn, Tl, Pb, and Bi nanoparticles have also been demonstrated by the detection of organic dyes and biomolecules [59–61].

Bismuth-based substrate

Bismuth is regularly found as a byproduct of mining copper, lead, and tin, and it is relatively cheap compared to rare metals. Despite being a heavy metal, bismuth is considered harmless because it is non-toxic and non-carcinogenic. This starkly contrasts other elements in the periodic table that are close to bismuth, such as arsenic, antimony, and lead, which are extremely toxic and hazardous to the environment [62]. Recently, bismuth has attracted a lot of attention as a scientific breakthrough for its potential use in biomedicine. Additionally, compared to other metals like silver, Bi is thought to be one of the non-reactive and biologically inert heavy metals, making it more appropriate for in vivo applications. Bi nanoparticles (NPs) and other form of Bi NPs such as bismuth oxyhalide, bismuth calcogenide containing oxide, sulfide, selenide and telluride, and over the last decade, it has significantly expanded in a variety of fields such as biosensor, tissue engineering, bioimaging, and photocatalyst etc. [63]. Moreover, bismuth shows tunable surface plasmon resonance near ultraviolet, visible, near IR region [64] which has drawn much attention in SERS applications. Now a days, Bi NPs, Bi thin film, composites

of bismuth oxyiodide (Au@BiOI), BiOI and BiOI-Au, heterostructure Ag@ZnO@Bi_2WO_6 substrates have demonstrated significant SERS activity [59, 65–69].

(d) Semiconductors

NiO was the first SERS semiconductor observed by Yamada and coworkers in 1982, in which an enhanced Raman signal of pyridine molecule adsorbed on nickel oxide was observed [70]. Later their group observed that TiO_2 had a similar enhancing effect [71]. Ueba reported a theoretical Raman scattering from adsorbed molecules onto ZnO and TiO2 surfaces in the same year [72]. After that, a wide variety of transition metal oxide was developed as SERS substrate with the explosive advancement of nanomaterials that have demonstrated huge enhancement greater than 10^6. Unlike the conventional SERS, it is anticipated to combine various resonance types, such as surface plasmon resonance, charge transfer, exciton, and molecular resonances [58]. As for the semiconductor substances, Raman enhancement is usually associated with the charge transfer mechanism due to the lack of electron density in the conduction band, which inhibits collective oscillations, and their band gaps and density of free electrons may be controlled in a multitude of ways. In contrast, it is challenging for coinage metals to have chemical effects because their electronic state is almost unchanged. Free electrons may exhibit an LSPR effect when exposed to certain stimulating light irradiation, which subsequently causes the EM enhancement characteristic, and their distinct optical, chemical, electrical, and catalytic capabilities, semiconductor materials give

conventional SERS new viability and could result in valuable activities [58, 73]. The enhancement in Raman signal by semiconducting materials has been the subject of several investigations up to this point categorized into two ways that the semiconductor material can be utilized to boost the Raman signals of adsorbed molecules: first, directly as a substrate; second, indirectly by acting as a "antenna" or "trap" to control the Raman signal produced by the SERS substrate. Some exciting applications based on semiconductors' distinct physical and chemical features have already been developed using semiconductor-based SERS technology [73].

(i) Metal oxides

Due to its physical and chemical characteristics, metal oxides are the most studied semiconductor in the SERS area. TiO2 (001) crystal and NiO (110) surface SERS activity was shown by Yamada et al. [57–58]. In SERS, the enhancement in signal caused by the CT stimulation of the analyte-substrate interface was due to the chemical bonding of pyridine nitrogen with NiO or TiO2 atomic sites [70–71]. Semiconductor-enhanced Raman scattering has brought impressive advancement due to the fast development of nanoscience and nanotechnology as ZnO, CuO etc. [37, 47, 73–74].

(ii) Metal heterostructure

In order to increase the ultra-high sensitivity and multifunctionality of SERS active substrates, semiconductors can be hybridized with plasmonic metal nanoparticles. To prepare heterostructures, transition metals, and Au and Ag are

frequently combined. Because Ag or Au has a stronger ability to increase Raman in regions of visible laser wavelength, semiconductor-noble metal heterostructures are most frequently studied [58]. In this research field, semiconductors and metals are put together either directly in touch or as a sandwich with molecules as bridges. The semiconductor thickness can be adjusted to alter the SERS performance of the heterostructure, and the semiconductors' shape can vary between nanoparticles, nano-rods, sheets, chains, and flower-like structures. Creating heterostructures with a metal core and a semiconductor shell is possible. Additionally, sandwiched Raman probes can be connected to synthetic metals and semiconductors. The composition of the metals, the probe molecules, and the assembly methods all have an impact on the charge transfer direction and the extra electromagnetic field, which in turn affects the amplification of molecules on semiconductor-based heterostructures [46, 58, 73] Molecules are later adsorbed on this kind of heterostructure with numerous contact modes after being decorated on large-scale semiconducting materials with small metal particles. These experimental results prompted a number of inquiries into the theoretical and experimental foundations of the surface-enhancement mechanism.

1.5 Reproducibility

The main aspect of enhancing SERS signals is their reproducibility, explicitly referring to the ability to display signals from various measurements within a predetermined error in the acceptable range of 20% for industrial substrates when measuring conditions are similar. But SERS has come under fire for being difficult to replicate in real-world settings, mostly because the EM increase is so

highly heterogeneous. In addition, a variety of additional elements, such as sample preparation and experimental circumstances, may influence the reproducibility of SERS signals in real studies [73-74]. Therefore, it is essential to look into their root causes and find solutions with a view to decrease the effects of these problems.

1.5.1 Uniformity of substrate

The uniformity of substrate is also an important parameter that play crucial role in applied field. Numerous techniques have been suggested for the fabrication of substrate for SERS as a resulting the advancement of nanotechnology. High reproducibility and consistency of the manufactured nanostructured substrates are provided by ordered geometric structure. Over the preceding two decades, incredible progress has been achieved in the development of nanostructures with well-defined morphologies and size distributions. Because of the homogenous distribution of nanomaterial on SERS substrates is produced a reliable SERS signal for quantitative measurement [73-74].

1.5.2 Stability of substrates

Raman probes on conventional substrates are easily photobleached and catalytic events occur closer to the metal surface, both of these phenomena have an impact on SERS activity [73, 75]. Nevertheless, research has shown that the surface of certain substrates can stabilize the pigment molecules, and their structural characteristics cause uniform probe molecule dispersion, favoring reliable and repeatable SERS spectra. The hot spots on SERS substrates' innate structural

instability are a vital factor in the repeatability of SERS. By melting or by surface atom diffusion initiated or accelerated by laser irradiation, the hot spots may experience structural changes that alter the nanoparticles' form, size, and inter-particle distance. Surface atoms diffuse more readily than atoms in the interior because they have a lower coordination number. For nanoparticles, which exhibit high enhancement factors due to anisotropic morphologies (such as nano-rods, stars, and cubes), surface diffusion is more likely to take place in order to lower their surface energy by rearranging the nanoparticles into a form that is more durable (spherical shape) [73]. This phenomenon may be prevented by reducing the laser power and exposure time or by altering the surface with the help of metal oxides, strong adsorbates, or other metal shells, which might stop this behavior. Compared to traditional metals, semiconductor materials, and their structures are thermodynamically more stable and cost-effective [73-74].

1.6 Characterization Techniques for SERS substrates

1.6.1 X-ray diffraction pattern (XRD)

X-ray diffraction patterns (XRD) is performed for analyse of the structural characteristics of the prepared materials. The XRD pattern is generated by the constructive interference of crystalline sample and monochromatic X-rays. Constructive interference was developed as a result of monochromatic X-rays of wavelength λ interacting with the materials and diffracted ray according to Bragg's Law which demonstrates that a crystalline sample's interplaner spacing (d),

diffraction angle (θ), and X-ray wavelength (λ) all relate to one another as given below [76],

$$n\lambda = 2d\sin\theta \quad (1.19)$$

Where, n = order of diffraction (n = 1, 2, 3.....), λ = wavelength of X-rays, d = spacing between two adjacent diffracting planes, θ = angle of diffraction.

Moreover, the Debye-Scherrer equation can be used to calculate the average crystallite size [76].

$$D = k\,\lambda\,\beta\cos\theta \quad (1.20)$$

Where, D represents the average crystallite size, k is the dimensionless value 0.9, λ is the X-ray wavelength, β shows the full width at half-maximum (FWHM), and Bragg's angle θ.

Using the high-resolution X-ray diffraction (HR-XRD) by Rigaku Smart Lab 9 kW, and Bench top XRD (BT-XRD) through the Rigaku Miniflex 600 Desktop X-Ray Diffraction System, the structure of the synthesized samples was recorded between the scan angle of 10^0 and 80^0, with Cu Kα radiation (λ = 1.5405 Å). Then observed XRD data was well matched with the standard data i.e. JCPDS card by International Center for Diffraction Data (ICDD).

1.6.2 Fourier Transform Infrared Spectroscopy (FT-IR)

On the Nicolet iS5 (THERMO Electron Scientific Instruments LLC), Fourier-transformed infrared spectra (FT-IR) were collected to investigate the functional

group present in the materials. The FT-IR spectrum was obtained in the region of 400-4000 cm^{-1}, and sampling was carried out using the KBr pelletization method.

1.6.3 Scanning Electron Microscopy (SEM)

Scanning electron microscope (SEM) is a type of electron microscopic technique that scans the surface to get information about the topography of the surface of small particles (μm to nm). The prepared materials' morphology was investigated using a scanning electron microscope (SEM) mounted with an EVO-MA15/18 scanning electron microscope.

1.6.4 X-ray Photo Electron Spectroscopy (XPS)

A surface sensitive technique X-ray photoelectron spectroscopy (XPS) is widely applied to identify the elemental composition and their chemical states in the sample.

Thermo Fisher Scientific's X-ray photoelectron spectroscopy (XPS) with K-Alpha radiation was used to determine the chemical composition of the prepared samples.

1.6.5 UV-Visible Spectroscopy

To identify the absorbance or reflectance band of any molecule, UV-Vis spectroscopy is a crucial instrument. It is an absorption spectroscopic technique that employs electromagnetic light with wavelengths between 200 and 800 nm. Agilent Cary 60 UV-visible spectrophotometer (UV-Vis spectrophotometer) was used to

analyze the optical properties of the prepared samples in aqueous solutions in the range of 200 to 800 nm.

1.6.6 Raman and SERS measurement

Raman and SERS spectra of all samples were measured using the Benchtop Raman spectrometer (Research India Raman spectrometer) with a 3648-pixel CCD detector. The excitation source for these measurements was a 785 nm diode laser. The laser power of 0.51 mW to 0.71 mW or 80–100 mW was used on the samples.

In addition, the α-300 Access (WITec, Germany) was used to record the Raman spectra using a confocal Raman spectrometer with a UHTS spectrometer equipped with a 600 nm grating, 50x microscope, and 532 nm, 633 nm laser excitation at about ~1.0 mW power. Raman spectrum data were subjected to baseline correction applying a polynomial approach and then visualized in Origin software.

1.7 Summary of the thesis

The thesis mainly focuses on exploring the SERS activity of new emerging non-noble metal, particularly Bismuth, using probe molecules such as dyes and some biologically essential molecules. Previous studies demonstrate that noble metals are readily oxidized and have less biocompatibility, and the SERS approach has used a rough metal surface to amplify the Raman signal from a scatter system close to the metal surface. Nanostructures of semiconductors with high thermal stability and plasmonic property have been a popular choice as a SERS substrate. The selection and preparation of traditional substrates are the most crucial factors to consider when

conducting a SERS experiment. An essential part of a SERS experiment is selecting and fabricating a conventional substrate. Chemical methods are commonly used over electrochemical or laser ablation methods for producing non-noble metal nanoparticles because they are less expensive, time-consuming, and laborious [58, 65].

Thus, the present work also focused on reducing the noble metal dependency as an alternative choice. we have applied several bismuth-based materials as a SERS substrate in the present work. SERS substrates were synthesized by hydrothermal or chemical precipitation methods. For the hydrothermal synthesis, a stainless steel autoclave with a Teflon coating served as the reaction vessel. The specifics of the materials synthesis are covered in the relevant experimental section of the chapters, and an overview of these domains is given as follows.

(1) Synthesis of bismuth heterostructure and bismuth oxides and employed as novel SERS substrate. The SERS activity was carried out using dye detection. Moreover, a bismuth heterostructure substrate was employed to investigate whether the standard probe PATP gave genuine SERS spectra or converted them to DMAB. These objectives are discussed and reported in the chapter 2.

(2) Chapter 3 deals with the synthesis of bismuth oxybromide ($Bi_{24}O_{31}Br_{10}$) and utilized as a substrate for SERS for the detection organic dyes (Methyl orange, Rhodamine B, and p-nitrophenol) and its activity was investigated in different solvents (water and ethanol).

(3) Preparation of AgBr-CTAB assisted bismuth oxybromide and the SERS activity was performed by detecting Rhodamine 6G and food colors. In addition, in situ SERS detection of Sudan I in chili powder was carried out using AgBr-CTAB assisted bismuth oxybromide and oxygen-rich bismuth oxybromide ($Bi_{24}O_{31}Br_{10}$) novel substrate, and the details are explained in chapter 4.

(4) Quantitative estimation of biomolecules such as an endogenous indole that is a physiologically active molecule Isatin and its derivative1-Methylisatin (1-Misa), 1-Phenylisatin (1-Phisa), 5-Flueroisatin (5-Fisa), 5-Idoisatin (5-Iisa), and neurotransmitter on bismuth based SERS substrate. Further studied the effect of pH in Isatin's and acetylcholine neurotransmitter biomolecules using the Raman and SERS, and briefly discussed in chapter 5.

References:

[1]R. R. Jones, D. C. Hooper, L. Zhang, D. Wolverson, and V. K. Valev, "Raman techniques: fundamentals and frontiers," *Nanoscale Res. Lett.*, vol. 14, pp. 1–34, 2019.

[2]A. Smekal, "Zur quantentheorie der dispersion," *Naturwissenschaften*, vol. 11, no. 43, pp. 873–875, 1923.

[3]C. V. Raman and K. S. Krishnan, "A new type of secondary radiation," *Nature*, vol. 121, no. 3048, pp. 501–502, 1928.

[4]G. Landsberg, "Eine neue Erscheinung bei der Lichtzerstreuung in Krystallen," *Naturwissenschaften*, vol. 16, p. 558, 1928.

[5]S.-L. Zhang, *Raman spectroscopy and its application in nanostructures*. John Wiley & Sons, 2012.

[6]B. S. Kademani, G. Surwase, and V. Kumar, "Raman spectroscopy research: a scientometric perspective," *Pearl A J. Libr. Inf. Sci.*, vol. 1, no. 4, pp. 46–66, 2007.

[7]R. S. Krishnan and R. K. Shankar, "Raman effect: History of the discovery," *J. Raman Spectrosc.*, vol. 10, no. 1, pp. 1–8, 1981.

[8]G. Keresztury, "R aman spectroscopy: Theory," *Handb. Vib. Spectrosc.*, 2006.

[9]"https://revistas.ufps.edu.co/index.php/ingenio/article/view/3308/4263."

[10] D. A. Long, *The raman effect*. John Wiley & Sons Ltd, 2002.

[11] R. L. McCreery, *Raman spectroscopy for chemical analysis*. John Wiley & Sons, 2005.

[12] J. R. Ferraro, *Introductory raman spectroscopy*. Elsevier, 2003.

[13] D. W. Ball, "Theory of Raman spectroscopy," *Spectroscopy*, vol. 16, no. 11, pp. 32–34, 2001.

[14] C. N. Banwell and E. M. McCash, *Fundamentals of Molecular Spectroscopy*. McGrawHill,1994.[Online]. Available:https://books.google.co.in/books?id=si8vAQAAIAAJ

[15] V. Ramanathan, "Raman, His Effect and Its Avatars," *Resonance*, vol. 26, pp. 1267–1278, 2021.

[16] Z. Deng and S. Mukamel, "Nonlinear susceptibilities and coherent and spontaneous Raman spectroscopy of polyatomic molecules in condensed phases," *J. Chem. Phys.*, vol. 85, no. 4, pp. 1738–1752, 1986.

[17] "Raman-Effect-Treatise.pdf (gauravtiwari.org)."

[18] K. Eberhardt, C. Stiebing, C. Matthäus, M. Schmitt, and J. Popp, "Advantages and limitations of Raman spectroscopy for molecular diagnostics: an update," *Expert Rev. Mol. Diagn.*, vol. 15, no. 6, pp. 773–787, 2015.

[19] D. C. Harris and M. D. Bertolucci, *Symmetry and spectroscopy: an introduction to vibrational and electronic spectroscopy*. Courier Corporation, 1989.

[20] A. Kudelski, "Analytical applications of Raman spectroscopy," *Talanta*, vol. 76, no. 1, pp. 1–8, 2008, doi: https://doi.org/10.1016/j.talanta.2008.02.042.

[21] M. Fleischmann, P. J. Hendra, and A. J. McQuillan, "Raman spectra of pyridine adsorbed at a silver electrode," *Chem. Phys. Lett.*, vol. 26, no. 2, pp. 163–166, 1974.

[22] P. A. Mosier-Boss, "Review of SERS substrates for chemical sensing," *Nanomaterials*, vol. 7, no. 6, p. 142, 2017.

[23] D. L. Jeanmaire and R. P. Van Duyne, "Surface Raman spectroelectrochemistry: Part I. Heterocyclic, aromatic, and aliphatic amines adsorbed on the anodized silver electrode," *J. Electroanal. Chem. interfacial Electrochem.*, vol. 84, no. 1, pp. 1–20, 1977.

[24] M. G. Albrecht and J. A. Creighton, "Anomalously intense Raman spectra of pyridine at a silver electrode," *J. Am. Chem. Soc.*, vol. 99, no. 15, pp. 5215–5217, 1977.

[25] K. Kneipp *et al.*, "Single molecule detection using surface-enhanced Raman scattering (SERS)," *Phys. Rev. Lett.*, vol. 78, no. 9, p. 1667, 1997.

[26] S. Nie and S. R. Emory, "Probing single molecules and single nanoparticles by surface-enhanced Raman scattering," *Science (80-.).*, vol. 275, no. 5303, pp. 1102–1106, 1997.

[27] D. Qi, L. Lu, L. Wang, and J. Zhang, "Improved SERS sensitivity on plasmon-free TiO2 photonic microarray by enhancing light-matter coupling," *J. Am.*

Chem. Soc., vol. 136, no. 28, pp. 9886–9889, 2014.

[28] M. Fan, G. F. S. Andrade, and A. G. Brolo, "A review on recent advances in the applications of surface-enhanced Raman scattering in analytical chemistry," *Anal. Chim. Acta*, vol. 1097, pp. 1–29, 2020.

[29] A. Hakonen, P. O. Andersson, M. S. Schmidt, T. Rindzevicius, and M. Käll, "Explosive and chemical threat detection by surface-enhanced Raman scattering: A review," *Anal. Chim. Acta*, vol. 893, pp. 1–13, 2015.

[30] E. Katz and I. Willner, "Integrated nanoparticle–biomolecule hybrid systems: synthesis, properties, and applications," *Angew. Chemie Int. Ed.*, vol. 43, no. 45, pp. 6042–6108, 2004.

[31] X. Li, G. Chen, L. Yang, Z. Jin, and J. Liu, "Multifunctional Au-coated TiO2 nanotube arrays as recyclable SERS substrates for multifold organic pollutants detection," *Adv. Funct. Mater.*, vol. 20, no. 17, pp. 2815–2824, 2010.

[32] N. L. Rosi and C. A. Mirkin, "Nanostructures in biodiagnostics," *Chem. Rev.*, vol. 105, no. 4, pp. 1547–1562, 2005.

[33] M. Moskovits, "Surface-enhanced spectroscopy," *Rev. Mod. Phys.*, vol. 57, no. 3, p. 783, 1985.

[34] M. Moskovits, "Surface-enhanced Raman spectroscopy: a brief retrospective," *J. Raman Spectrosc. An Int. J. Orig. Work all Asp. Raman Spectrosc. Incl. High. Order Process. also Brillouin Rayleigh Scatt.*, vol. 36, no. 6-7, pp. 485–496, 2005.

[35] A. Otto, I. Mrozek, H. Grabhorn, and W. Akemann, "Surface-enhanced Raman scattering," *J. Phys. Condens. Matter*, vol. 4, no. 5, p. 1143, 1992.

[36] J. Langer *et al.*, "Present and future of surface-enhanced Raman scattering," *ACS Nano*, vol. 14, no. 1, pp. 28–117, 2019.

[37] G. C. Schatz, M. A. Young, and R. P. Van Duyne, "Electromagnetic Mechanism of SERS BT - Surface-Enhanced Raman Scattering: Physics and Applications," K. Kneipp, M. Moskovits, and H. Kneipp, Eds. Berlin, Heidelberg: Springer Berlin Heidelberg, 2006, pp. 19–45. doi: 10.1007/3-540-33567-6_2.

[38] M. Jahn *et al.*, "Plasmonic nanostructures for surface enhanced spectroscopic

methods," *Analyst*, vol. 141, no. 3, pp. 756–793, 2016.

[39] J. Gersten and A. Nitzan, "Electromagnetic theory of enhanced Raman scattering by molecules adsorbed on rough surfaces," *J. Chem. Phys.*, vol. 73, no. 7, pp. 3023–3037, 1980.

[40] A. Campion and P. Kambhampati, "Surface-enhanced Raman scattering," *Chem. Soc. Rev.*, vol. 27, no. 4, pp. 241–250, 1998.

[41] M. Moskovits, "Surface roughness and the enhanced intensity of Raman scattering by molecules adsorbed on metals," *J. Chem. Phys.*, vol. 69, no. 9, pp. 4159–4161, 1978.

[42] S.-Y. Ding, E.-M. You, Z.-Q. Tian, and M. Moskovits, "Electromagnetic theories of surface-enhanced Raman spectroscopy," *Chem. Soc. Rev.*, vol. 46, no. 13, pp. 4042–4076, 2017.

[43] J. A. Creighton, C. G. Blatchford, and M. G. Albrecht, "Plasma resonance enhancement of Raman scattering by pyridine adsorbed on silver or gold sol particles of size comparable to the excitation wavelength," *J. Chem. Soc. Faraday Trans. 2 Mol. Chem. Phys.*, vol. 75, no. 0, pp. 790–798, 1979, doi: 10.1039/F29797500790.

[44] K. L. Kelly, E. Coronado, L. L. Zhao, and G. C. Schatz, "The optical properties of metal nanoparticles: the influence of size, shape, and dielectric environment," *The Journal of Physical Chemistry B*, vol. 107, no. 3. ACS Publications, pp. 668–677, 2003.

[45] P. L. Stiles, J. A. Dieringer, N. C. Shah, and R. P. Van Duyne, "Surface-enhanced Raman spectroscopy," *Annu. Rev. Anal. Chem.*, vol. 1, pp. 601–626, 2008.

[46] X. X. Han, W. Ji, B. Zhao, and Y. Ozaki, "Semiconductor-enhanced Raman scattering: Active nanomaterials and applications," *Nanoscale*, vol. 9, no. 15, pp. 4847–4861, 2017.

[47] L. K. Ausman and G. C. Schatz, "On the importance of incorporating dipole reradiation in the modeling of surface enhanced Raman scattering from spheres," *J. Chem. Phys.*, vol. 131, no. 8, 2009.

[48] W. Li *et al.*, "CuTe nanocrystals: shape and size control, plasmonic properties, and use as SERS probes and photothermal agents," *J. Am. Chem. Soc.*, vol. 135, no. 19, pp. 7098–7101, 2013.

[49] S. Hayashi, R. Koh, Y. Ichiyama, and K. Yamamoto, "Evidence for surface-enhanced Raman scattering on nonmetallic surfaces: Copper phthalocyanine molecules on GaP small particles," *Phys. Rev. Lett.*, vol. 60, no. 11, p. 1085, 1988.

[50] C. Zhan, X.-J. Chen, Y.-F. Huang, D.-Y. Wu, and Z.-Q. Tian, "Plasmon-mediated chemical reactions on nanostructures unveiled by surface-enhanced Raman spectroscopy," *Acc. Chem. Res.*, vol. 52, no. 10, pp. 2784–2792, 2019.

[51] Y.-F. Huang, H.-P. Zhu, G.-K. Liu, D.-Y. Wu, B. Ren, and Z.-Q. Tian, "When the signal is not from the original molecule to be detected: chemical transformation of para-aminothiophenol on Ag during the SERS measurement," *J. Am. Chem. Soc.*, vol. 132, no. 27, pp. 9244–9246, 2010.

[52] Y. Wang, X. Zou, W. Ren, W. Wang, and E. Wang, "Effect of silver nanoplates on Raman spectra of p-aminothiophenol assembled on smooth macroscopic gold and silver surface," *J. Phys. Chem. C*, vol. 111, no. 8, pp. 3259–3265, 2007.

[53] Y.-F. Huang *et al.*, "Surface-enhanced Raman spectroscopic study of p-aminothiophenol," *Phys. Chem. Chem. Phys.*, vol. 14, no. 24, pp. 8485–8497, 2012.

[54] Y. Wang *et al.*, "Pt-based nanostructures for observing genuine SERS spectra of p-aminothiophenol (PATP) molecules," *Appl. Sci.*, vol. 7, no. 9, p. 953, 2017.

[55] X. Tian, L. Chen, H. Xu, and M. Sun, "Ascertaining genuine SERS spectra of p-aminothiophenol," *Rsc Adv.*, vol. 2, no. 22, pp. 8289–8292, 2012.

[56] E. C. Le Ru, E. Blackie, M. Meyer, and P. G. Etchegoin, "Surface enhanced Raman scattering enhancement factors: a comprehensive study," *J. Phys. Chem. C*, vol. 111, no. 37, pp. 13794–13803, 2007.

[57] Z.-Q. Tian, B. Ren, and D.-Y. Wu, "Surface-enhanced Raman scattering: from noble to transition metals and from rough surfaces to ordered nanostructures," *The Journal of Physical Chemistry B*, vol. 106, no. 37. ACS Publications, pp. 9463–9483, 2002.

[58] X. Han and B. Zhao, "Surface-enhanced Raman scattering (SERS) and applications," in *Molecular and Laser Spectroscopy*, Elsevier, 2020, pp. 349–386.

[59] A. G. Bezerra *et al.*, "Plasmonics and SERS activity of post-transition metal nanoparticles," *J. Nanoparticle Res.*, vol. 20, no. 5, p. 142, 2018, doi: 10.1007/s11051-018-4249-8.

[60] S. K. Jha, Z. Ahmed, M. Agio, Y. Ekinci, and J. F. Löffler, "Deep-UV Surface-Enhanced Resonance Raman Scattering of Adenine on Aluminum Nanoparticle Arrays," *J. Am. Chem. Soc.*, vol. 134, no. 4, pp. 1966–1969, Feb. 2012, doi: 10.1021/ja210446w.

[61] P. C. Wu *et al.*, "Demonstration of Surface-Enhanced Raman Scattering by Tunable, Plasmonic Gallium Nanoparticles," *J. Am. Chem. Soc.*, vol. 131, no. 34, pp. 12032–12033, Sep. 2009, doi: 10.1021/ja903321z.

[62] J. M. Bothwell, S. W. Krabbe, and R. S. Mohan, "Applications of bismuth (III) compounds in organic synthesis," *Chem. Soc. Rev.*, vol. 40, no. 9, pp. 4649–4707, 2011.

[63] M.-A. Shahbazi *et al.*, "The versatile biomedical applications of bismuth-based nanoparticles and composites: therapeutic, diagnostic, biosensing, and regenerative properties," *Chem. Soc. Rev.*, vol. 49, no. 4, pp. 1253–1321, 2020, doi: 10.1039/C9CS00283A.

[64] J. Toudert, R. Serna, and M. Jiménez de Castro, "Exploring the Optical Potential of Nano-Bismuth: Tunable Surface Plasmon Resonances in the Near Ultraviolet-to-Near Infrared Range," *J. Phys. Chem. C*, vol. 116, no. 38, pp. 20530–20539, Sep. 2012, doi: 10.1021/jp3065882.

[65] A. G. Bezerra, P. Cavassin, T. N. Machado, T. D. Woiski, R. Caetano, and W. H. Schreiner, "Surface-enhanced Raman scattering using bismuth nanoparticles: a study with amino acids," *J. Nanoparticle Res.*, vol. 19, no. 11, 2017, doi: 10.1007/s11051-017-4057-6.

[66] R. M. Philip and D. B. Mohan, "Effect of varied laser powers on Raman spectra of bismuth thin films fabricated for developing a stable SERS platform," in *AIP*

[67]R. Balaji *et al.*, "Fabricating BiOI nanostructures armed catalytic strips for selective electrochemical and SERS detection of pesticide in polluted water,"

Environ. Pollut., vol. 296, p. 118754, 2022, doi: https://doi.org/10.1016/j.envpol.2021.118754.

[68] M. D. Prasad, M. G. Krishna, and S. K. Batabyal, "Facet-Engineered Surfaces of Two-Dimensional Layered BiOI and Au–BiOI Substrates for Tuning the Surface-Enhanced Raman Scattering and Visible Light Photodetector Response," *ACS Appl. Nano Mater.*, vol. 2, no. 6, pp. 3906–3915, Jun. 2019, doi: 10.1021/acsanm.9b00771.

[69] I. Korkmaz *et al.*, "Fabrication of superhydrophobic Ag@ZnO@Bi2WO6 membrane disc as flexible and photocatalytic active reusable SERS substrate,"*J. Mol. Struct.*, vol. 1223, p. 129258, 2021, doi:https://doi.org/10.1016/j.molstruc.2020.129258.

[70] H. Yamada, Y. Yamamoto, and N. Tani, "Surface-enhanced raman scattering (SERS) of adsorbed molecules on smooth surfaces of metals and a metal oxide," *Chem. Phys. Lett.*, vol. 86, no. 4, pp. 397–400, 1982.

[71] H. Yamada and Y. Yamamoto, "Surface enhanced Raman scattering (SERS) of chemisorbed species on various kinds of metals and semiconductors," *Surf. Sci.*, vol. 134, no. 1, pp. 71–90, 1983.

[72] H. Ueba, "Theory of raman scattering from molecules adsorbed at semiconductor surfaces," *Surf. Sci.*, vol. 131, no. 2–3, pp. 328–346, 1983.

[73] W. Ji, B. Zhao, and Y. Ozaki, "Semiconductor materials in analytical applications of surface-enhanced Raman scattering," *J. Raman Spectrosc.*, vol. 47, no. 1, pp. 51–58, 2016.

[74] D. Bokov *et al.*, "Nanomaterial by Sol-Gel Method: Synthesis and Application," *Adv. Mater. Sci. Eng.*, vol. 2021, p. 5102014, 2021, doi: 10.1155/2021/5102014.

[75] A. I. Pérez-Jiménez, D. Lyu, Z. Lu, G. Liu, and B. Ren, "Surface-enhanced Raman spectroscopy: benefits, trade-offs and future developments," *Chem. Sci.*, vol. 11, no. 18, pp. 4563–4577, 2020.

[76] B. D. Cullity, *Elements of X-ray Diffraction*. Addison-Wesley Publishing, 1956.